Transcriptome analysis reveals the genetic basis underlying the development of skin appendages and immunity in hedgehog(Atelerix albiventris)

Hui-Ming Li
Guangdong Institute of Applied Biological Resource
Bi-Ze Yang
Guangdong Institute of Applied Biological Resource
Xiu-Juan Zhang
Guangdong Institute of Applied Biological Resource
Hai-Ying Jiang
Guangdong Institute of Applied Biological Resource
Lin-Miao Li
Guangdong Institute of Applied Biological Resource
Hafiz Ishaq Ahmad
Guangdong Institute of Applied Biological Resource
Jinping Chen (chenjp@giabr.gd.cn)
Guangdong Institute of Applied Biological Resources https://orcid.org/0000-0002-0808-6617

Research

Keywords: hedgehog, skin appendage, adaptive evolution, RNA-Seq, molecular biology

Posted Date: May 7th, 2020

DOI: https://doi.org/10.21203/rs.3.rs-25069/v1

Version of Record: A version of this preprint was published at Scientific Reports on August 18th, 2020.
See the published version at https://doi.org/10.1038/s41598-020-70844-y.

Transcriptome analysis reveals the genetic basis underlying the development of skin appendages and immunity in hedgehog (*Atelerix albiventris*)

Hui-Ming Li[1], Bi-Ze Yang[1], Xiu-Juan Zhang[1], Hai-Ying Jiang[1], Lin-Miao Li[1], Hafiz Ishaq Ahmad[1], Jin-Ping Chen[1*]

[1]Guangdong Key Laboratory of Animal Conservation and Resource Utilization, Guangdong Public Laboratory of Wild Animal Conservation and Utilization, Guangdong Institute of Applied Biological Resources, Guangdong Academy of Science, Guangzhou 510260, China

*Corresponding author: chenjp@giabr.gd.cn

Abstract

Background: The expression of hair features is an evolutionary adaptation resulting from interactions between many organisms and their environment. Elucidation of the mechanisms that underlie the expression of such traits is a topic in evolutionary biology research; however, the genetic basis of skin appendage development and differentiation remains poorly understood. Therefore, we assessed the *de novo* transcriptome of the hedgehog (*Atelerix albiventris*) at three developmental stages and compared gene expression profiles between abdomen hair and dorsal spine tissues.

Results: We identified 328,576 unigenes in our transcriptome, among which 3,598 were differentially expressed between hair- and spine-type tissues. We identified 3 keratin genes related to hair and spine development through comparative analysis of tissues before and after growth of skin appendages. Dorsal and abdomen skin tissues 5 days after birth were compared and the resulting differentially expressed genes (DEGs) were mainly enriched in keratin

filament, intermediate filament, epithelium cell differentiation, and epidermis development based on GO enrichment analysis, and tight junction, p53, and cell cycle signaling pathways based on KEGG enrichment analysis. Expression variations of *MBP8, SFN, Wnt10, KRT1*, and *KRT2* may be the main factors regulating hair and spine differentiation for the hedgehog. Strikingly, DEGs in hair-type tissues were also significantly enriched in immune-related terms and pathways with hair-type tissues exhibiting more upregulated immune genes than spine-type tissues. Thus, we propose that spine development was an adaptation that provided protection against injuries or stress and reduced hedgehog vulnerability to infection.

Conclusion: Our study provided a list of potential genes involved in the regulation of skin appendage development and differentiation in *A. albiventris*. This is the first transcriptome survey of hair traits for a non-model mammal species, and the candidate genes provided here may provide valuable information for further studies of skin appendages and skin disorder treatments.

Keywords: hedgehog, skin appendage, adaptive evolution, RNA-Seq, molecular biology

Background

Perceiving and responding to life-threatening signals and regulating their own morphological characteristics constitute a fundamental challenge for all mammals. Evolution has shaped the ability of organisms to adapt skin appendages to increase their chances of survival. Accordingly, a variety of appendages have evolved on the skin of mammals, either to assist organisms in carrying out specific behaviors or to protect them from predators and pathogenic bacteria [1,2].

Compared with animals that possess passive defense adaptations such as feathers, scales, etc., the hedgehog has evolved into an unusual, nocturnal, spine-covered mammal [3]. Spines

potentiate attacking power and enhance the role of skin appendages as a defense mechanism. The hedgehog progresses through a series of well-defined stages during its life cycle, from embryonic, to non-spine, to with-spine stages. These transitions are governed by tightly regulated gene expression at pre-transcriptional, epigenetic, and translational levels. Spine- and hair-type skin tissues from the hedgehog thus offer a natural model to analyze the genomic basis for the evolution of epidermal appendage formation.

Development of hair follicles on a skin appendage with a complex growth cycle is characterized by anagen, catagen, and telogen stages, and many key signaling pathways and genes are involved in their regulation [4–6]. According to many studies, the WNT/β-catenin signaling pathway in the dermis may be the first dermal signal [7–9]. Sonic hedgehog (SHH) is another secreted protein in the follicular placode that plays a major part in epithelial-mesenchymal signaling [10,11]. SHH depends on WNT signaling and is required for the proliferation of follicular epithelium and development of dermal condensate into dermal papilla [4]. In addition, many key genes related to skin appendage development have been identified; *TGFaR* (epidermal growth factor receptor) and transcription factor *ETS2* regulate hair follicle shape and are responsible for hair follicle architecture and wavy hair [12,13], and *HOXC13* and *KRT75* control hair shaft differentiation [14–17]. Further, *EDA* and *EDAR* interact with members of the bone morphogenetic protein (BMP) family, some of which inhibit follicle development to establish follicle patterning [2,18–20].

The abovementioned studies primarily focused on mammalian hairs and scales; little is known about changes in gene expression during the development of spine appendages in mammals. Therefore, we aimed to perform a detailed analysis of the transcriptome of skin from abdomen hair and dorsal spines of the hedgehog (*Atelerix albiventris*) by comparing groups of transcripts

differentially expressed at different hedgehog developmental stages. We identified key candidate genes related to the development and differentiation of skin appendages whose importance should be verified in future studies. Nonetheless, the presented novel information will be widely applicable in many fields, such as skin disease and skin immune genes, and provide insight into the molecular mechanisms of skin appendage development in general.

Results

Illumina sequencing and *de novo* assembly

To identify the transcriptome and molecular mechanisms governing skin appendage development and differentiation, we analyzed temporal changes in transcript abundance of *A. albiventris* (Fig. 1a). RNA sequencing generated 82.2 ± 6.0 G (mean ± SD) read pairs for 16 skin tissue samples (Supplementary Table 1). After quality trimming, 96.8 ± 0.4% of reads were retained, indicating a high-quality dataset (>90% reads with ≥Q30). The *de novo* assembly using Trinity revealed 328,576 unigenes, which were used for subsequent analysis. We evaluated biological reproducibility by individually comparing biological replicates through principle component analysis (PCA) (Fig. 1b). As expected, similar gene expression patterns in both hair- and spine-type samples were observed. PCA analysis also demonstrated more separation between the two skin appendage types. A neural network graph based on self-organizing feature map (SOM) analysis revealed dynamic transcriptional changes at the individual stages of appendage development in *A. albiventris* (Fig. 1c).

Functional annotation and classification of unigenes

Use of the NR and Swiss-Prot databases yielded reliable protein annotations for approximately 42% of unigenes. Absolute unigenes were annotated using seven major public protein databases (Table 1), of which the greatest number of matches (68.3%) was obtained using the

NT database. Of 328,576 unigenes assembled, 243,444 genes (74.1%) exhibited a positive match against at least one database. Thus, our gene annotation results from *A. albiventris* transcriptome were considered high quality.

In our study, 70,833 unigenes were assigned to 56 sub-categories of GO terms belonging to the following three main categories: biological process (BP), cellular component (CC), and molecular function (MF). These main categories included 26, 20, and 10 sub-term categories, respectively (Fig. 2). The most enriched GO terms were related to cellular and metabolic processes (BP), cell and organelle (CC), and binding and catalytic activity (MF). Importantly, we found some GO terms (level 4) in the BP category related to skin appendage development and differentiation, including (positive/negative) regulation of cell differentiation, regulation of cell proliferation, reproductive structure development, cell development, and ovarian follicle cell development.

In addition, we annotated all unigenes using KEGG pathway analysis to understand their top-level function and role in the hedgehog biological system. Overall, 36,283 unigenes were mapped to 232 biological pathways clustered in 5 KO hierarchies in the functional ortholog system. Among these KO hierarchies, 15 unique KEGG pathways represented cellular processes (A) and 30, 22, 98, and 72 pathways represented environmental information processing (B), genetic information processing (C), metabolism (D), and organismal systems (E), respectively (Fig. 3). The largest KO group was translation (5743 unigenes, 13%), followed by signal transduction (5551 unigenes, 12.6%), and endocrine system (3223 unigenes, 7.3%). Further, a small proportion of unigenes were annotated in the B category of signal transduction related to skin appendage development and differentiation, including Rap1 (814 unigenes), Wnt (355 unigenes), Hippo (626 unigenes), TGF-β (206 unigenes), and Notch (171

unigenes) signaling pathways.

Analysis of differentially expressed genes in skin appendage tissues

Analysis of DEGs in skin appendage tissues finally identified 3,598 DEGs in the three developmental stages, and 816 DEGs shared by the two types of tissues (Fig. 4a-c). As shown in the Venn diagram (Fig. 4d), more DEGs were found in tissues with spines (HH1Y and HS1Y) than in tissues without spines (HH1N and HS1N).

To validate expression patterns indicated by the transcriptome data, 11 differentiation-related DEGs were selected for RT-qPCR analysis including *KRT2*, *LEF1*, *RSPO2*, *ARRB*, *TGFB2*, *GRB2*, *SFN*, *TCF7*, *CTNNB1*, *HOXC13*, and *WIF1* (Supplementary Table 2). Expression trends determined by RT-qPCR significantly correlated with the RNA-Seq data (Fig. 5a). Expression of these 11 genes at the three developmental stages was also analyzed, revealing expression patterns similar to those determined by RNA-sequencing (Fig. 5b). Expression of *LEF1*, *TGFB2*, *SFN*, and *WIF1* at stages I–III increased significantly. However, expression of *KRT1* and *RSPO2* gradually decreased. Overall, both approaches confirmed the observed DEG trend patterns, indicating the accuracy of the transcriptome data and *de novo* RNA-Seq data.

Differentially expressed genes related to skin appendage development

In order to further understand the spine development mechanism of the hedgehog, we conducted DEG analysis before and after spine development. In total, 28 DEGs were identified between HS1N and HS1Y, among them, 11 genes were downregulated, and the remaining 17 genes were upregulated (Supplementary Table 3). Based on GO and KEGG annotation, we found one downregulated gene of unknown open reading frame (LOC103122410) related to cell differentiation and multi-cellular organismal development in the BP category, and one

downregulated keratin-associated protein like gene (LOC103118355) related to keratin filament.

In order to identify genes that activate the development of hedgehog abdominal hair, we analyzed DEGs before and after the occurrence of abdominal hair. A total 82 DEGs were identified between HH1N and HH1Y, of which 62 genes were downregulated, and the remaining 20 genes were upregulated (Supplementary Table 4). Notably, LOC103122410 was also present in these DEGs; in addition, keratin gene *KRT2* was highly expressed in HH1Y. We speculate that these genes play an important role in activating the development of hedgehog abdominal hair and spines.

Differentially expressed genes related to skin appendage differentiation

We identified 1,517 DEGs by comparing the gene expression profiles of spine- (HS5) and hair-type (HH5) tissues in *A. albiventris* five days after birth. We screened 2 genes related to cell differentiation (*NOTCH* and keratin-associated protein (*KRTAP*) 9-2), 18 genes related to cell proliferation (*TGFB1, FGF, KRT2, TCHH, BMP3, BMP8, APOA1,CCDC85A, INHBB, MICAL2, VSIG8, FCN, GDF5, DMD, GDNF, FAT1, CSF*, and *GDF15*), and many keratin-related genes (*KRT1, KRT2*, *KRTAP*, etc). These genes might be indicative of hedgehog transcriptome involvement in spine and hair differentiation.

Based on annotation of the *A. albiventirs* transcripts with the GO database, the DEGs were significantly enriched in keratin-related terms. Keratin filament is an important component of skin appendages; the main DEGs involved in this process included *KRT1, KRT2, MYH, DES, BMP8, SHH*, and several *KRTAP* genes (Fig. 6a, b). In addition, *CSTA* was involved in the biological process of keratinocyte differentiation. In a directed acyclic graph diagram

associated with this term, cell differentiation, epithelial cell differentiation, and epidermis development were enriched, and the main DEGs involved in this process included *KRT1, KRT2, MBP8, FGF, Wnt10*, and *MYH* (Fig. 6b). The only significantly enriched KEGG pathways among all DEGs comparing HH5 and HS5 tissues were tight junction and p53 signaling pathways (Fig. 6c; Table 2). In addition, eight pathways related to skin appendage development and differentiation were enriched, including cell cycle, MAPK, Rap1, Hippo, VEGF, TGF-beta, and PPAR signaling pathways. It is noteworthy that *SFN, BMP8, Wnt3, Wnt10, MYH*, and *SFN* were found in both annotation results, suggesting they are closely related to differentiation of keratinocytes and epidermal cells.

In our data, keratin-related genes were highly abundant and also significantly overexpressed in the dorsal spine-type tissues. In the hedgehog transcriptome, more than 3,000 transcripts were annotated to 6 keratin genes (*KRT1, KRT2, KRT5, KRT10, TCHP*, and *CHRNA1*) and approximately 20 keratin-associated proteins. Through alignment of *KRT1* gene sequences from 20 species, we found that the hedgehog *KRT1* gene sequence has a deletion of 45 bp compared with other species (Fig. 6d). The two hedgehog species were isolated into one clade in the bayesian phylogenetic tree (Fig. 6e), suggesting that *KRT1* may be one of the important regulatory genes for the development and differentiation of hedgehog skin appendages.

Immune-related genes in epidermis of hedgehog

In this study, we also found many immune-related genes comparing HH5 and HS5. After KEGG enrichment analysis, we found no significant enrichment of immune-related pathways in spine-type tissues, and fewer immune-related pathways and genes than in hair-type tissues. Hair-type tissues exhibited 19 enriched immune-related pathways, three of which were significantly enriched, and 47 transcripts annotated with 32 immune-related genes (Fig. 7a,b).

200 In addition, we observed similar GO enrichment analysis results. The number of terms and
201 genes enriched in hair-type tissues was significantly higher than in spine-type tissues, of which
202 two of the seven terms were significantly enriched, and 25 transcripts were annotated with 11
203 immune-related genes (Fig. 7c,d).
204
205 **Discussion**
206 The genetic basis of morphological variation, both within and between species, provides a
207 major topic in evolutionary biology. In mammals, the development of skin appendages such as
208 hair, tooth, and scale involves complex interactions between the epidermis and the underlying
209 mesenchyme as part of an established hierarchical morphogenetic process [21]. Specifically,
210 mammals develop a coat containing many distinct types of hair. Such diversity is associated
211 with molecular and signaling pathways that drive formation and induction in a specific spatial
212 and temporal manner [22]. Reciprocal interactions between epithelial and mesenchymal tissues
213 constitute a central mechanism that determines the location, size, and shape of organs [23].
214
215 In the current study, we aimed to explore the genetic basis for hedgehog skin appendage
216 differentiation and development and the resulting expression of the spine trait. We identified
217 328,576 unigenes in our transcriptome, all of which were annotated in 7 databases (Table 1).
218 Taken together, our *de novo* assemblies revealed higher quality compared with previous studies
219 [24,25] that formed the foundation of all our subsequent analyses. According to GO and KEGG
220 annotation analysis, a total of 70,833 and 36,238 unigenes were mapped to 56 sub-categories
221 and 232 biological pathways, respectively (Fig. 2,3). We identified some of the key pathways
222 involved in skin development; these annotations may provide a valuable resource for further
223 understanding the specific functions and pathways in *A. albiventris*.
224

225 Newborn hedgehogs begin to develop hair/spines approximately two hours after birth. We
226 found 6 shared genes (*APOE, COX2, COX3, FCN, RP-L11e, SH3GL*) through analysis of
227 DEGs before and after hair/spine development, indicating that these genes are essential
228 regulatory genes in the development of skin appendages, whether hair or spine. Further, we
229 compared the gene expression profiles of spine- and hair-type tissues to systematically assess
230 key regulatory genes for spine and hair differentiation in *A. albiventris*. *SFN*, upregulated in
231 spine-type tissues, is a regulator of mitotic translation that interacts with a variety of translation
232 and initiation factors [26], is enriched in the p53 signaling pathway, and has a role in
233 keratinocyte differentiation and skin barrier establishment in the BP category (GO). *SFN* plays
234 an important role in maintaining hair follicle development, especially affecting the formation
235 of hair shaft structure [27]. Bu *et al*. (2014) determined that SFN gene and protein were
236 significantly highly expressed in the thicker, longer, and harder skin of wool, indicating that
237 *SFN* was involved in the regulation of wool character development [28]. In addition, we
238 identified *FGF* as the upregulated DEG enriched in the MAPK and Rap1 signaling pathways.
239 These pathways often act together by forming signaling loops during organogenesis [29] and
240 induce the most fundamental biological processes, such as the formation of periodic patterns.
241 Hebert *et al.* (1994) demonstrated that *FGF* plays an important role in regulation of the hair
242 cycle growth, and functions as an inhibitor of hair elongation by promoting progression from
243 anagen stage, the growth phase of the hair follicle, to catagen stage, the apoptosis-induced
244 regression phase [16]. Hence, we believe that *SFN* and *FGF* may be important regulators that
245 affect spine development and differentiation in *A. albiventris*.
246
247 We also compared *KRT1* gene sequences of 20 mammals with that of the hedgehog, in which
248 we identified a 45-bp deletion in the latter. Keratins, the major structural proteins of epithelia,
249 are a diverse group of cytoskeletal scaffolding proteins that form intermediate filament

networks and provide structural support to keratinocytes that maintain skin integrity [30]. In general, *KRT1* is highly conserved in mammals, however, molecular defects in keratin intermediate filament-related genes can cause keratinocyte and tissue-specific fragility, accounting for a large number of genetic disorders in skin and its appendages [31,32]. Therefore, whether the deletion phenomenon in hedgehog *KRT1* has special significance for spine development and differentiation in the hedgehog warrants further research and verification.

Lastly, we analyzed immune-related genes in the skin transcriptome of *A. albiventris*. We found that hair-type skin had more immune-related genes than spine-type skin. Choo *et al.* (2016) found that interferon epsilon (*IFNE*), which was exclusively expressed in epithelial cells and was important to mucosal immunity, was pseudogenized in pangolins. They proposed that scale development provided protection against injuries or stress and reduced pangolin vulnerability to infection, thus protection by scales on the pangolin body compensated for the low immunity of this species to a certain extent [33]. From our current data, we speculate that there may be significant differences in the immune function of skin with different appendage types, and that the occurrence of spines may be an innovative physical protection for dorsal skin with relatively low immunity.

Conclusions

In the current study, we conducted a comprehensive transcriptome analysis of *A. albiventris* to explore the genetic basis for the growth of skin appendages. Transcriptome analysis provided a rich list of unigenes expressed in hair- and spine-type tissues at three different developmental stages, of which 328,576 unigenes and 3,598 DEGs were identified. Candidate genes were identified that are likely involved in the regulation of hair and spine growth and differentiation.

The knowledge acquired in this study of the molecular and signaling pathways related to hair and spine expression greatly contributes to the current genetic resources for the hedgehog and mammalian species that harbor shaggy appendages, as well as traits that could be potentially exploited for curing skin diseases of other animals, even humans.

Methods

Ethics statement

All animal procedures in the study were approved by the ethics committee for animal experiments at the Guangdong Institute of Applied Biological Resources (reference number G2ABR20170523) and followed basic principles. We confirm that all methods were performed in accordance with relevant guidelines and regulations.

Biological samples

According to observations of the growth characteristics of hedgehogs, hairs and spines on the back and abdomen begin to appear approximately two hours after birth; therefore we obtained 8 hedgehogs at 3 different stages of appendage development from a commercial animal farm (Dongguan City, China). Hedgehog hair (HH) and spine (HS) tissues were collected from 2 specimens within 2 h of birth (Stage I, HH1N/HS1N), 3 specimens after 2 h but within the first birth day (Stage II, HH1Y/HS1Y), and 3 specimens 5 days after birth (Stage III, HH5/HS5). For collection of skin appendages, animals were first anesthetized with diethyl ether and then killed via cervical dislocation. Sixteen skin tissue samples representing the two types of appendages (abdomen hair-type and dorsal spine-type) were rapidly excised, immediately snap-frozen on dry ice, and stored at –80 °C until RNA extraction.

RNA extraction and RNA-seq

Total RNA from each tissue sample was extracted using the RNeasy Kit (Qiagen, Hilden, Germany). RNA purity was determined using a NanoPhotometer® spectrophotometer (Implen, Inc., Westlake Village, CA, USA). All unigenes were annotated using the basic local alignment search tool (BLASTX), considering hits with e-values of 1E−5 against seven databases: NCBI non-redundant protein sequences (Nr); NCBI non-redundant nucleotide sequences (Nt); Protein family (Pfam) database; Clusters of Orthologous Groups of Proteins (KOG/COG) database; Swiss-Prot (a manually annotated and reviewed protein sequence database); KEGG Ortholog (KO) database; Gene Ontology (GO) database. Differentially expressed genes (DEGs) were identified by comparing gene expression levels between samples (or sample groups). Bowtie2 [34] was used to align clean reads with all unigenes and RSEM [35] was used to calculated gene expression levels for each sample. Differential gene expression was analyzed using DESeq270 V1.16.1 in RStudio71 V1.0.143 running R72 V3.4.1. All sequencing was conducted by Novogene (Beijing, China).

Quantitative real-time reverse-transcription PCR (RT-qPCR)

RNA was extracted from skin appendage tissue samples using TRIzol reagent (Invitrogen, Carslbad, CA, USA). Then, cDNA was synthesized using the Toyobo reverse-transcription kit (Toyobo, Osaka, Japan). Eleven genes related to hair and/or spine development were selected for analysis based on functional annotation data, and fluorescent qPCR primers were designed accordingly (Supplementary Table 2). RT-qPCR was performed in a 20-μL reaction volume, with four technical replicates for each sample, using the TransStart® Top Green qPCR SuperMix kit (TransGen Biotech, Beijing, China). Relative gene expression levels were analyzed using the 2^(-ΔΔCT) method (Bustin *et al*. 2010). PCR conditions were as follows: pre-denaturation at 95 °C for 10 min; 40 cycles of 15 s at 95 °C (denaturation), 30 s at 58 °C (annealing), and 20 s at 72 °C (extension); and a final melting curve stage from 60-95 °C to

verify the specificity of the amplicons.

Phylogenetic analysis

KRT1 sequence authenticity was verified by BLAST search in GenBank (Supplementary Table 5). Sequences were edited using MAFFT v 6.81b [36] and Mesquite [37]. MRMODELTEST v.2.3 [38] was used to select the best-fit model of nucleotide substitution under the Akaike information criterion (AIC) [39]. Bayesian inference of phylogeny was performed using BEAST v 1.6.1 [40] with default settings except for GRT+I+G model. An uncorrelated relaxed clock fixed to lognormal distribution was employed as the site model using a Yule speciation tree prior sampled every 10,000th generation for 100 million generations. Effective sample seizes (ESS) were verified using Tracer v1.5 and a consensus tree was constructed in TreeAnnotator v1.6.1 with 20% burn-in. For the concatenated dataset, all parameters were estimated independently for each partition and displayed using FigTree v1.4.2. (http://www.geospiza.com/finchtv).

Abbreviations

A. albiventris, Atelerix albiventris; Hiseq, high-throughput sequencing; PCA, principal component analysis; KRT, keratin; FGF, fibroblast growth factor; SHH, sonic hedgehog; BMP, bone morphogenetic protein; DEGs, differentially expressed genes; RT-qPCR, quantitative real time polymerase chain reaction; SOM, self-organizing feature map

Declarations

Ethics approval and consent to participate

All animal procedures were approved by the ethics committee for animal experiments at the Guangdong Institute of Applied Biological Resources (reference number G2ABR20170523)

and followed basic principles.

Consent for publication

Not applicable

Availability of data and materials

Data analyzed in the current study are included within the article and its supplementary material. All unigene sequences from *A. albiventris* have been deposited in the GenBank Sequence Read Archive (SRA) under accession number PRJNA561241 for SUB6195278. We have uploaded supplemental material to figshare via the GSA Portal. Supplementary Table 1 contains the summary of sequencing statistics for the transcriptomes; Supplementary Table 2 contains the summary of primer information used in real-time PCR analysis; Supplementary Table 3 contains the differentially expressed genes between HS1N and HS1Y; Supplementary Table 4 contains the differentially expressed genes between HH1N and HH1Y; Supplementary Table 5 contains the species name and NCBI serial numbers of 19 additional species for phylogenetic analysis.

Competing interests

The authors declare that they have no competing interests or other interests that might be perceived to influence the results and/or discussion reported in this paper.

Funding

This study was supported by the GDAS' Project of Science and Technology Development (2019GDASYL-0103062), China Postdoctoral Science Foundation (2019M652832), and the GDAS' Special of Science and Technology Development (2018GDASCX-0107).

Authors' contributions

H. Li and J. Chen designed research; H. Li analyzed data and wrote the report; B. Yang developed software necessary to perform and record experiments; L. Li, X. Zhang, H. Ahmad, and H. Jiang provided expertise and advice on computational analysis; all authors edited the report.

Acknowledgments

We gratefully acknowledge the assistance of Professor Gang Li in the design of the experiments. We thank Wiley publishing (http://wileyeditingservices.com) for editing the draft of this manuscript.

Author details

1 Guangdong Key Laboratory of Animal Conservation and Resource Utilization, Guangdong Public Laboratory of Wild Animal Conservation and Utilization, Guangdong Institute of Applied Biological Resources, Guangzhou 510260, China

References

1. Gandolfi B, Outerbridge CA, Beresford LG, Myers JA, Pimentel M, Alhaddad H, et al. The naked truth: Sphynx and Devon Rex cat breed mutations in KRT71. Mamm Genome. 2010;21:509–515.

2. Di-Poï N, Milinkovitch MC. The anatomical placode in reptile scale morphogenesis indicates shared ancestry among skin appendages in amniotes. Sci Adv. 2016;2:1–9.

3. Zeller M, Reusch TBHTBH, Lampert W. A comparative population genetic study on calanoid freshwater copepods: investigation of isolation-by-distance in two Eudiaptomus species with a different potential for dispersal. Limnol Oceanogr. 2006;51:117–124.

400 4. Millar SE. Molecular mechanisms regulating hair follicle development. J Invest Dermatol.
401 2002;118:216–225.
402 5. Paus R, Mu S, Veen C Van Der, Maurer M, Eichmu S, Ling G. A Comprehensive Guide for
403 the Recognition and Classification of Distinct Stages of Hair Follicle. J Invest Dermatol.
404 1999;113:523–532.
405 6. Won HI, Schulze TT, Clement EJ, Watson GF, Watson SM, Rosalie C, et al. De novo
406 Assembly of the Burying Beetle Nicrophorus orbicollis (Coleoptera : Silphidae)
407 Transcriptome Across Developmental Stages with Identification of Key Immune Transcripts.
408 J Genomics. 2018;6:41–52.
409 7. Noramly S, Freeman A, Morgan BA. Beta-Catenin Signaling Can Initiate Feather Bud
410 Development. Development. 1999;126:3509–3521.
411 8. Andl T, Reddy ST, Gaddapara T, Millar SE. WNT signals are required for the initiation of
412 hair follicle development. Dev Cell. 2002;2:643–653.
413 9. Tsai SY, Sennett R, Rezza A, Clavel C, Grisanti L, Zemla R, et al. Wnt/β-catenin signaling
414 in dermal condensates is required for hair follicle formation. Dev Biol. Elsevier;
415 2014;385:179–188.
416 10. Bitgood MJ, McMahon AP. Hedgehog and Bmp genes are coexpressed at many diverse
417 sites of cell-cell interaction in the mouse embryo. Dev Biol. 1995;172:126–138.
418 11. Iseki S, Araga A, Ohuchi H, Nohno T, Yoshioka H, Hayashi F, et al. Sonic hedgehog is
419 expressed in epithelial cells during development of whisker, hair, and tooth. Biochem Biophys
420 Res Commun. 1996;218:688–693.
421 12. Luetteke NC, Qiu TH, Peiffer RL, Oliver P, Smithies O, Lee DC. TGFα deficiency results
422 in hair follicle and eye abnormalities in targeted and waved-1 mice. Cell. 1993;73:263–278.
423 13. Yamamoto H, Flannery ML, Kupriyanov S, Pearce J, McKercher SR, Henkel GW, et al.
424 Defective trophoblast function in mice with a targeted mutation of Ets2. Genes Dev.

425 1998;12:1315–1326.
426 14. Godwin AR, Capecchi MR. Hoxc13 mutant mice lack external hair. Genes Dev.
427 1998;12:11–20.
428 15. Potter CS, Pruett ND, Kern MJ, Baybo MA, Godwin AR, Potter KA, et al. The nude mutant
429 gene Foxn1 Is a HOXC13 regulatory target during hair follicle and nail differentiation. J Invest
430 Dermatol. 2011;131:828–837.
431 16. Cadieu E, Neff MW, Quignon P, Walsh K, Chase K, Parker HG, et al. Coat variation in the
432 domestic dog is governed by variants in three genes. Science (80-). 2009;326:150–153.
433 17. Koch PJ, Sundberg JP, Roop DR, Jaeger K, Den Z, Chen J. Mice Expressing a Mutant
434 Krt75 (K6hf) Allele Develop Hair and Nail Defects Resembling Pachyonychia Congenita. J
435 Invest Dermatol [Internet]. Elsevier Masson SAS; 2007;128:270–279.
436 18. Mou C, Jackson B, Overbeek PA, Schneider P, Headon DJ. Generation of the primary hair
437 follicle pattern. Proc Natl Acad Sci. 2006;103:9075–9080.
438 19. Pummila M, James MJ, Jaatinen R, Schneider P, Mikkola ML, Thesleff I, et al.
439 Ectodysplasin has a dual role in ectodermal organogenesis: inhibition of Bmp activity and
440 induction of Shh expression. Development. 2006;134:117–125.
441 20. Kamberov YG, Wang S, Tan J, Gerbault P, Wark A, Tan L, et al. Modeling recent human
442 evolution in mice by expression of a selected EDAR variant. Cell. Elsevier Inc.; 2013;152:691–
443 702.
444 21. Duverger O, Morasso MI. Epidermal Patterning and Induction of Different Hair Types
445 during Mouse Embryonic Development. Birth Defects Res C Embryo. 2009;87:263–272.
446 22. Hardy MH. The secret life of the hair follicle. Trends Genet. 1992;8:55–861.
447 23. Laurikkala J, Pispa J, Jung H-S, Nieminen P, Mikkola M, Wang X, et al. Regulation of hair
448 follicle development by the TNF signal ectodysplasin and its receptor Edar. Development.
449 2002;129:2541–2553.

450 24. Qiao L, Yang W, Fu J, Song Z. Transcriptome Profile of the Green Odorous Frog (Odorrana
451 margaretae). PLoS One. 2013; 8:e75211. DOI: 10.1371/journal.pone.0075211.
452 25. Shao Y, Wang LJ, Zhong L, Hong ML, Chen HM, Murphy RW, et al. Transcriptomes
453 reveal the genetic mechanisms underlying ionic regulatory adaptations to salt in the crab-eating
454 frog. Sci Rep. 2015;5:17551.
455 26. Kim S, Wong P, Coulombe PA. A keratin cytoskeletal protein regulates protein synthesis
456 and epithelial cell growth. Nature. 2006;441:362–365.
457 27. Owens P, Bazzi H, Engelking E, Han G, Christiano AM, Wang XJ. Smad4-dependent
458 desmoglein-4 expression contributes to hair follicle integrity. Dev Biol. 2008;322:156–166.
459 28. Bu R, Li J, Liu KD, Liu JF, Liu N. Study on the differential expression of the SFN gene in
460 fine-wool sheep. Heilongjiang Anim Sci Veterianary Med. 2014;10:80–83.
461 29. Jung HS, Francis-West PH, Widelitz RB, Jiang TX, Ting-Berreth S, Tickle C, et al. Local
462 inhibitory action of BMPs and their relationships with activators in feather formation:
463 Implications for periodic patterning. Dev Biol. 1998;196:11–23.
464 30. Chamcheu JC, Siddiqui IA, Syed DN, Adhami VM, Liovic M, Mukhtar H. Keratin gene
465 mutations in disorders of human skin and its appendages. Arch Biochem Biophys [Internet].
466 Elsevier Inc.; 2011;508:123–137.
467 31. Toivola DM, Boor P, Alam C, Strnad P. Keratins in health and disease. Curr Opin Cell
468 Biol. 2015;32C:73–81.
469 32. Magin TM, Vijayaraj P, Leube RE. Structural and regulatory functions of keratins. Exp
470 Cell Res. 2007;313:2021–2032.
471 33. Choo SW, Rayko M, Tan TK, Hari R, Komissarov A, Wee WY, et al. Pangolin genomes
472 and the evolution of mammalian scales and immunity. Genome Res. 2016;26:1312–1322.
473 34. Langmead B, Salzberg S. Langmead B, Salzberg SL. Fast gapped-read alignment with
474 Bowtie 2. Nat Methods. 2012;9:357–359.

35. Li B, Dewey CN. RSEM : accurate transcript quantification from RNA-Seq data with or without a reference genome. Bioinformatics. 2011;12:323–325.

36. Katoh K, Asimenos G, Toh H. Multiple alignment of DNA sequneces with MAFFT. Methods Mol Biol. 2009;537:39–64.

37. Maddison WP. Mesquite: a molecular system for evolutionary analysis. Evolution (N Y). 2009;62:1103–1118.

38. Nylander JA. MrModeltest v2. Evol. Biol. Center, Uppsala Univ. 2004.

39. Posada D, Crandall KA. MODELTEST: testing the model of DNA substitution. Bioinformatics. 1998;14:817–819.

40. Bouckaert R, Heled J, Kühnert D, Vaughan T, Wu CH, Xie D, et al. BEAST 2: A Software Platform for Bayesian Evolutionary Analysis. PLoS Comput Biol. 2014;10.

Tables, figures, supplementary tables

Figure 1 Phenotypes of skin appendages from 3 developmental stages of *Atelerix albiventris*. (a) Different phenotypes from 3 different developmental stages of *A. albiventris*; (b) Principal components analysis (PCA); (c) Gene expression-specific and phenotype-specific gene-trait correlation analysis based on self-organizing feature map module analysis.

Figure 2 Gene Ontology classification of assembled unigenes in *Atelerix albiventris*.

Figure 3 KEGG classification of assembled unigenes in *Atelerix albiventris*. (A) cellular

processes; (B) environmental information processing; (C) genetic information processing; (D) metabolism, (E) organismal systems.

Figure 4 Differential expression analysis of hair- and spine-type tissues in *Atelerix albiventris*. Volcano plot of DEGs for (a) 'HH1N vs HS1N', (b) 'HH1Y vs HS1Y', (c) 'HH5 vs HS5'. (d) Venn diagram showing co-DEGs among different tissues in *Atelerix albiventris.* DEGs, differentially expressed genes.

Figure 5 Quantitative real-time PCR analysis. (a) qPCR confirmation of 10 DEGs identified by RNA-seq in stage III tissues; (b) Relative expression levels of 10 DEGs in tissues at 3 developmental stages. Bars represent the relative expression levels of unigenes in stage III tissues normalized with respect to the internal control GAPDH. Error bars represent the standard error of three biological replicates. DEGs, differentially expressed genes.

Figure 6 KEGG and GO enrichment analysis of DEGs related to differentiation of KRT1 gene. (a,b) Directed acyclic graph related to skin appendage development and differentiation in GO enrichment analysis. (c) Dot plots of enriched KEGG pathways. (d) Multiple sequence alignment of *KRT1* gene from 20 species. (e) Bayesian phylogenetic tree with *KRT1* sequences from 20 species. DEGs, differentially expressed genes.

Figure 7 KEGG and GO enrichment analysis of DEGs related to immunity. (a,b) up- and downregulated KEGG signaling pathways and key genes related to immunity. (c,d) up- and downregulated GO terms and key genes related to immunity. DEGs, differentially expressed genes.

Table 1 Summary of functional annotations of assembled unigenes with public protein databases

Table 2 Candidate pathways and genes related to development and differentiation of spine and hair

Supplementary Table 1 Sample IDs for transcriptome sequencing

Supplementary Table 2 Summary of primers for real-time PCR analysis

Supplementary Table 3 Differentially expressed genes between HS1N and HS1Y

Supplementary Table 4 Differentially expressed genes between HH1N and HH1Y

Supplementary Table 5 NCBI accession numbers of *KRT1* sequences from 19 species

Figures

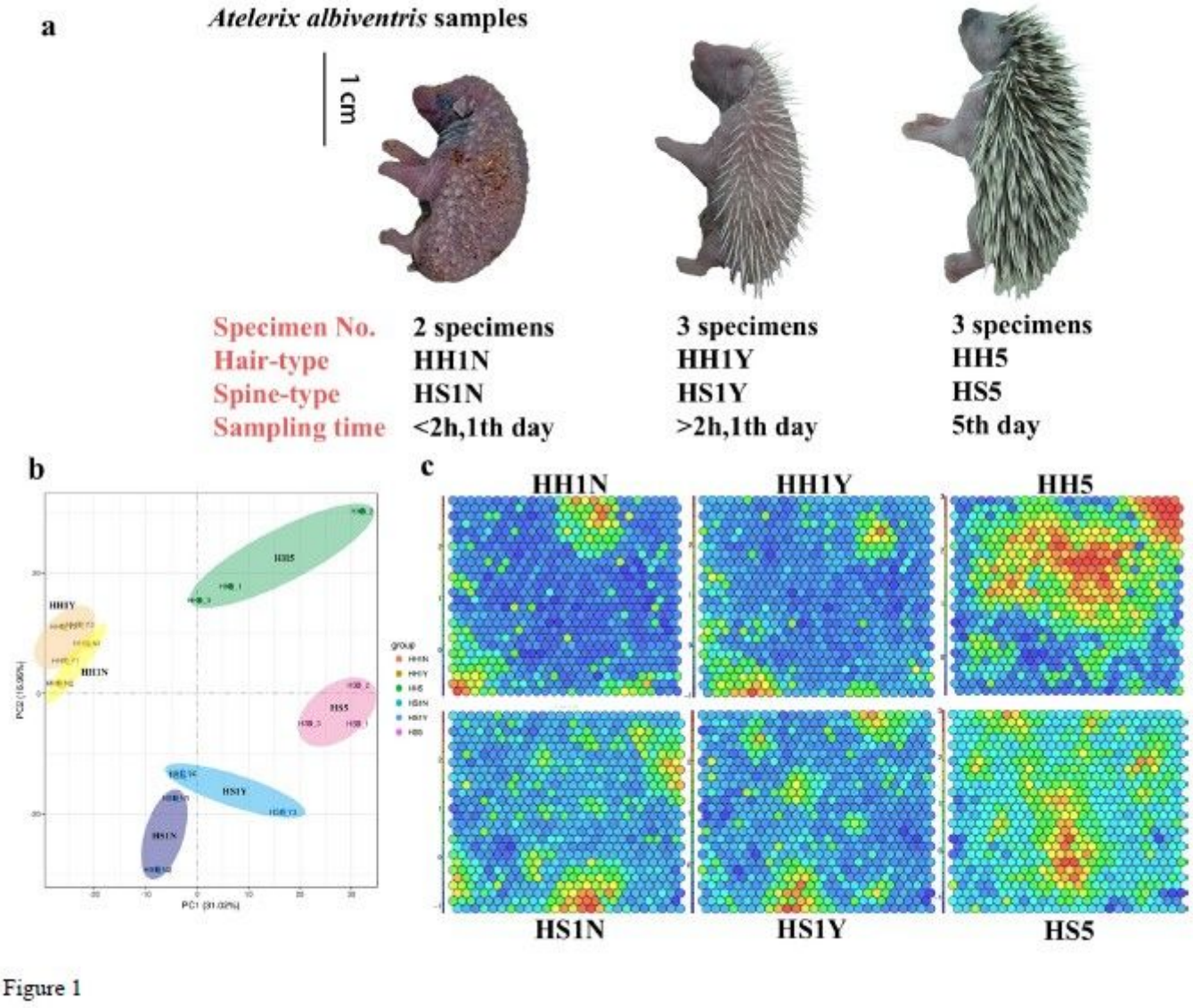

Figure 1

Figure 1

Phenotypes of skin appendages from 3 developmental stages of Atelerix albiventris. (a) Different phenotypes from 3 different developmental stages of A. albiventris; (b) Principal components analysis (PCA); (c) Gene expression-specific and phenotype-specific gene-trait correlation analysis based on self-organizing feature map module analysis.

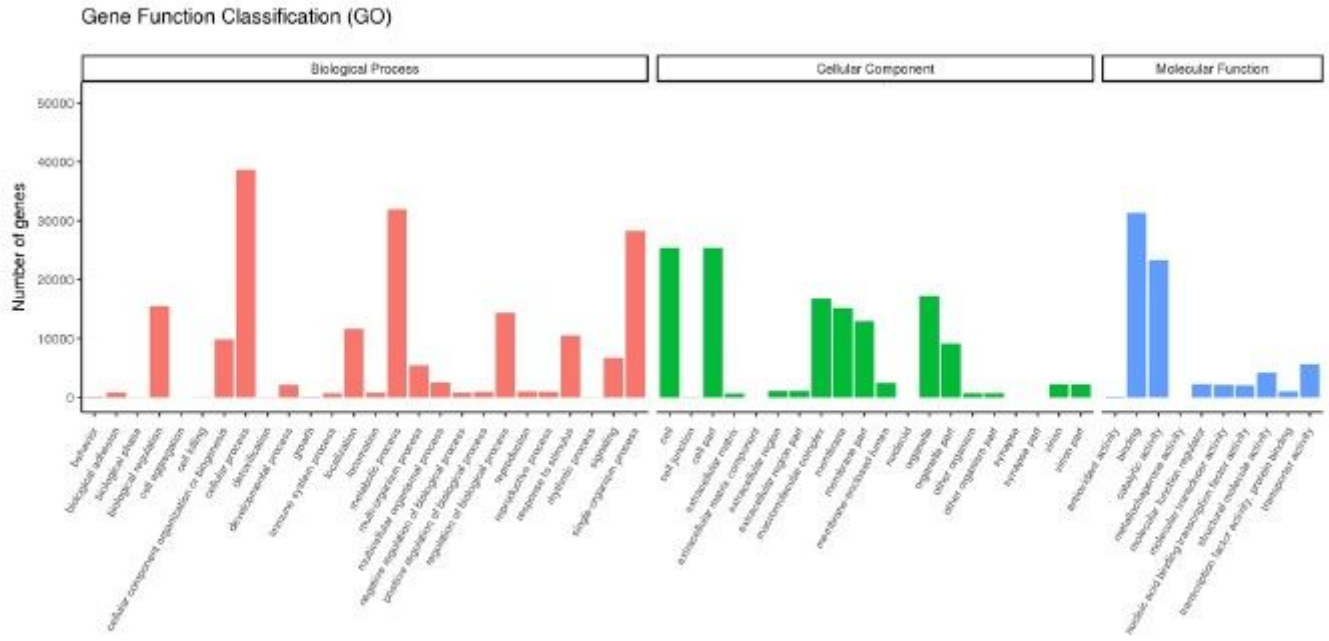

Figure 2

Figure 2

Gene Ontology classification of assembled unigenes in Atelerix albiventris.

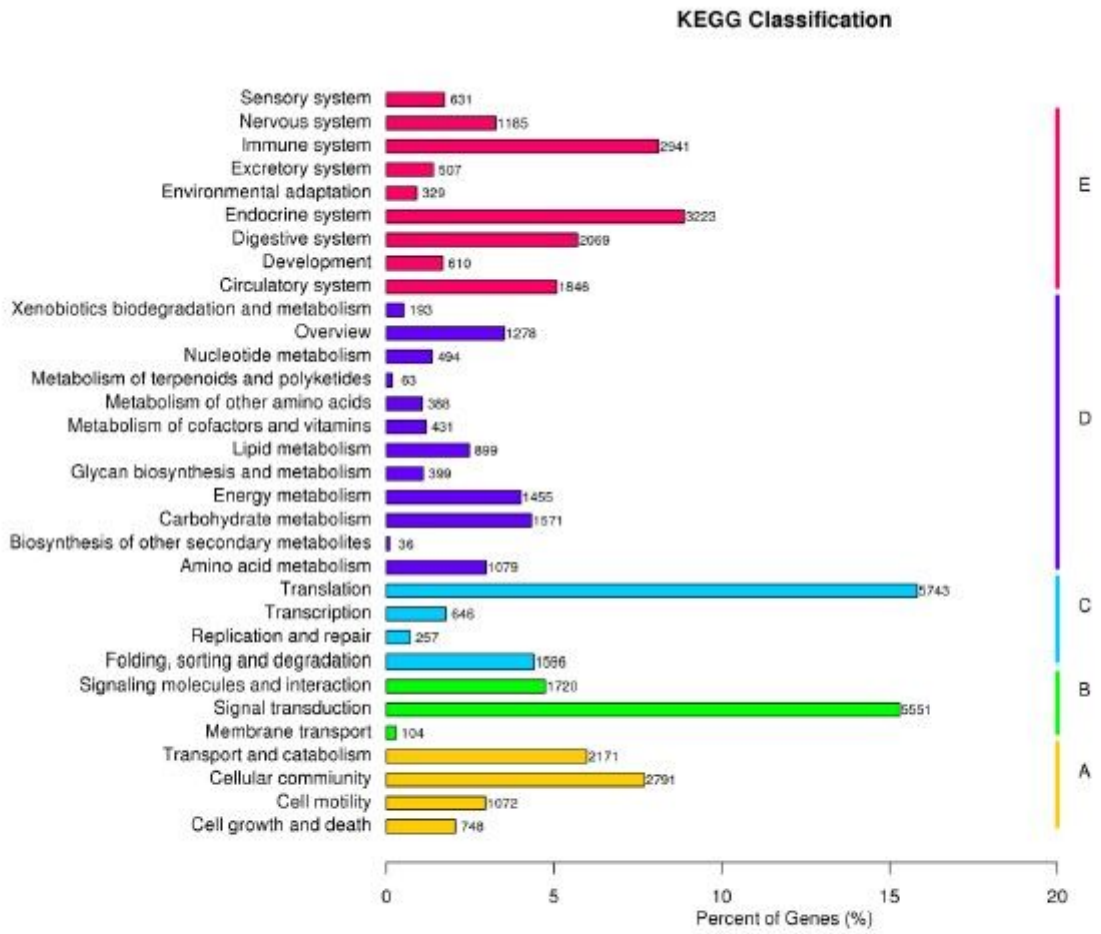

Figure 3

Figure 3

KEGG classification of assembled unigenes in Atelerix albiventris. (A) cellular processes; (B) environmental information processing; (C) genetic 500 information processing; (D) metabolism, (E) organismal systems.

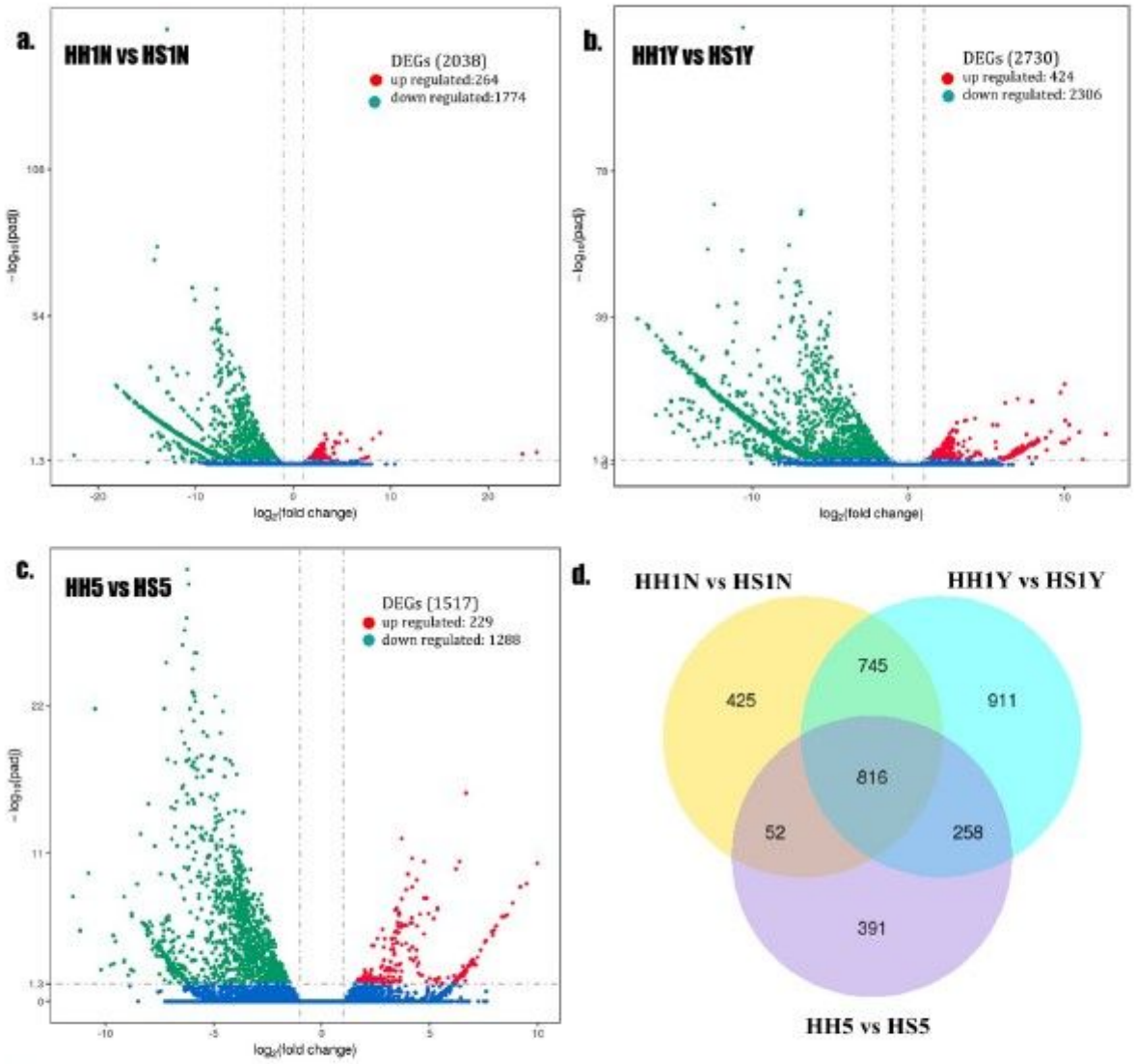

Figure 4

Figure 4

Differential expression analysis of hair- and spine-type tissues in Atelerix albiventris. Volcano plot of DEGs for (a) 'HH1N vs HS1N', (b) 'HH1Y vs HS1Y', (c) 'HH5 vs HS5'. (d) Venn diagram showing co-DEGs among different tissues in Atelerix albiventris. DEGs, differentially expressed genes.

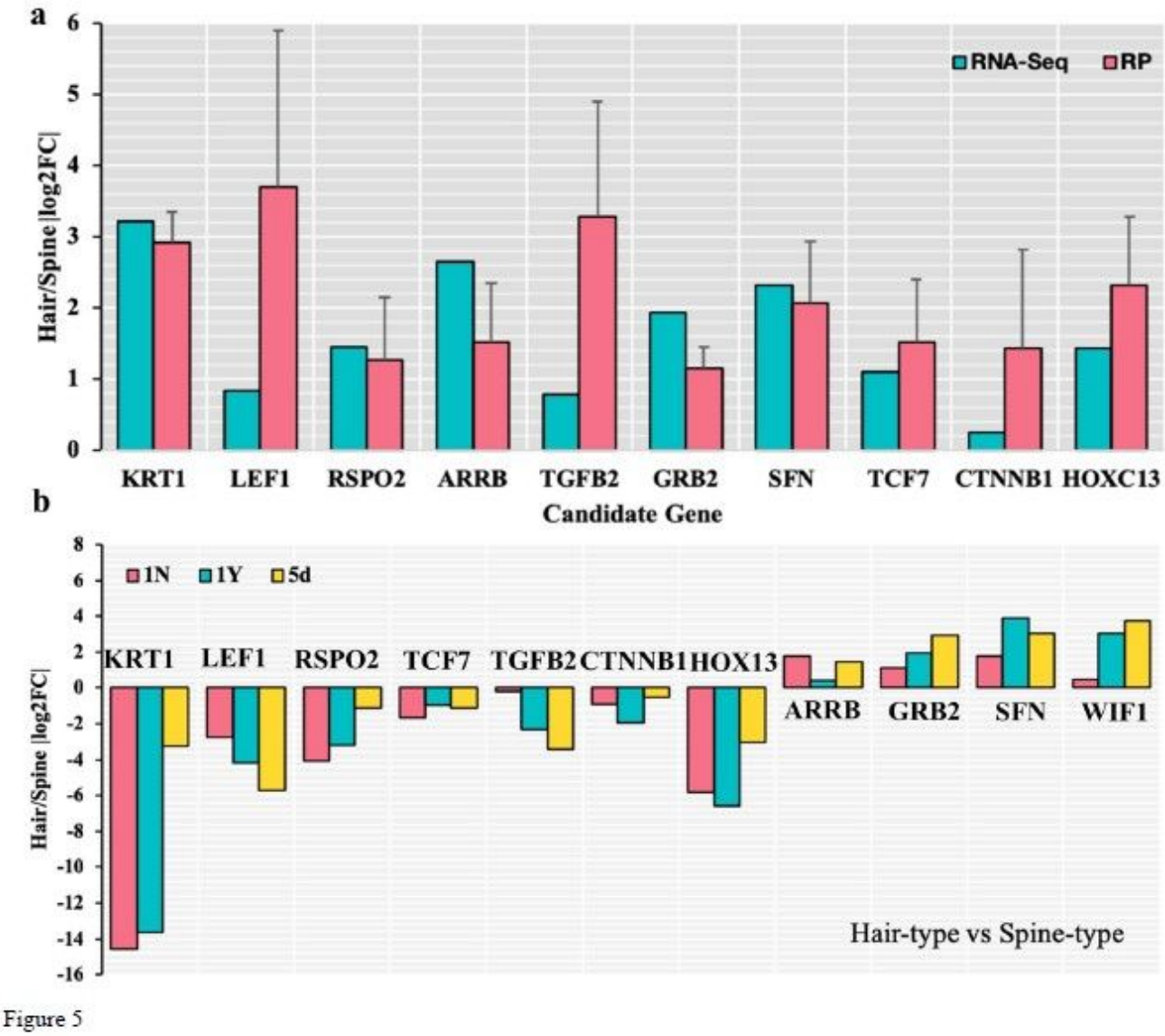

Figure 5

Figure 5

Quantitative real-time PCR analysis. (a) qPCR confirmation of 10 DEGs identified by RNA-seq in stage III tissues; (b) Relative expression levels of 10 DEGs in tissues at 3 developmental stages. Bars represent the relative expression levels of unigenes in stage III tissues normalized with respect to the internal control GAPDH. Error bars represent the standard error of three biological replicates. DEGs, differentially expressed genes.

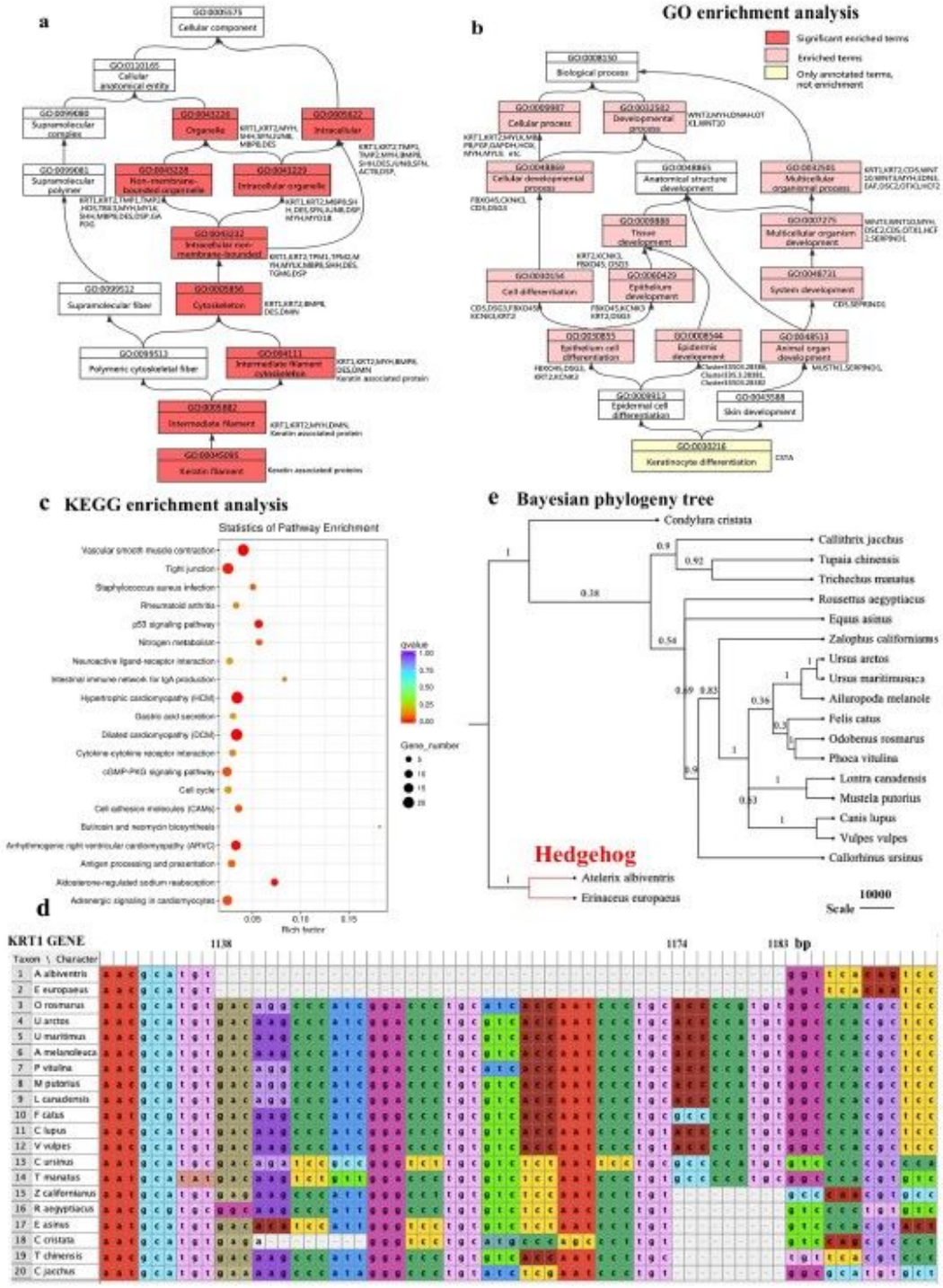

Figure 6

Figure 6

KEGG and GO enrichment analysis of DEGs related to differentiation of KRT1 gene. (a,b) Directed acyclic graph related to skin appendage development and differentiation in GO enrichment analysis. (c) Dot plots of enriched KEGG pathways. (d) Multiple sequence alignment of KRT1 gene from 20 species. (e) Bayesian phylogenetic tree with KRT1 sequences from 20 species. DEGs, differentially expressed genes.

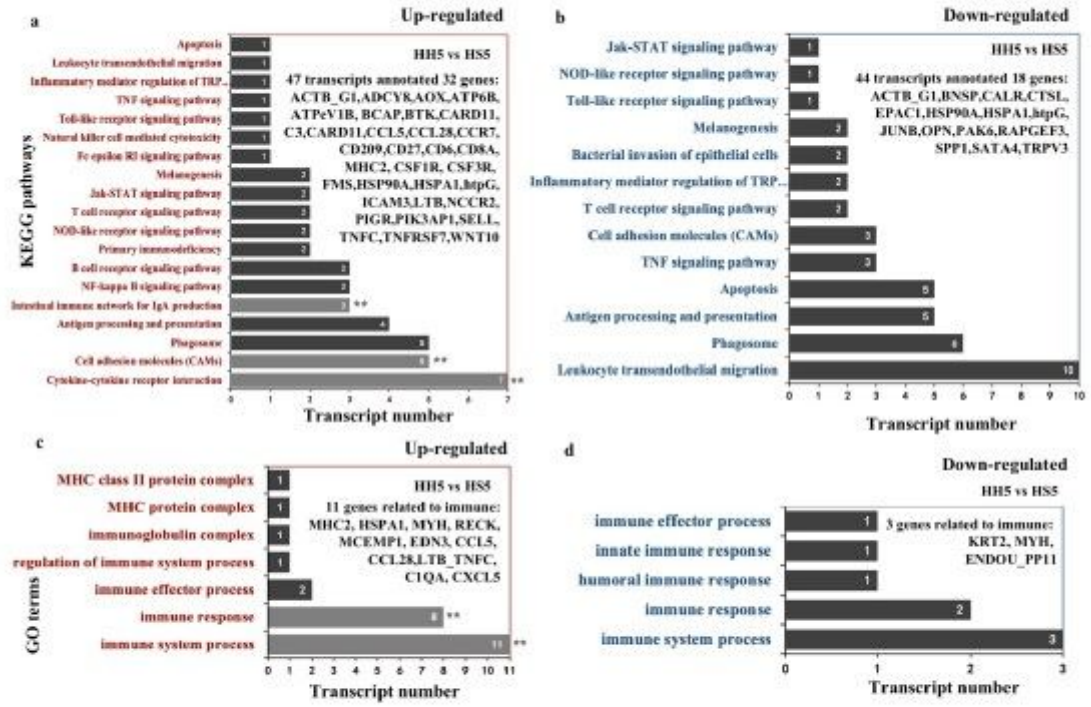

Figure 7

Figure 7

KEGG and GO enrichment analysis of DEGs related to immunity. (a,b) up- and downregulated KEGG signaling pathways and key genes related to immunity. (c,d) up- and downregulated GO terms and key genes related to immunity. DEGs, differentially expressed genes.

Supplementary Files

This is a list of supplementary files associated with this preprint. Click to download.

- SUPPLEMENTARYTABLE15.pdf
- TABLES12.pdf
- TABLES12.pdf
- SUPPLEMENTARYTABLE15.pdf